New Silicon and Germanium Frameworks by High-Pressure Synthesis

Ulrich Schwarz, Ulrich Burkhardt, Michael Hanfland[1], Katrin Meier, Carola J. Müller, Walter Schnelle, and Aron Wosylus

Frameworks of elemental germanium

The elements germanium and silicon can adopt several three-dimensional open framework structures at ambient condition. Recently, the novel clathrate-type element modification Ge(*cF*136) was synthesized by mild oxidation of Zintl phases [1]. The open framework nature of the new allotrope and the four-bonded character of the germanium atoms motivated an investigation of the pressure-induced structural changes of this unique atomic arrangement.

In-situ X-ray diffraction experiments with the diamond anvil cell technique were realized in-house and at a synchrotron source (ESRF) revealing a continuous compression of Ge(*cF*136) between ambient pressure and 12.7 GPa. Additional diffraction lines indicate the onset of a transformation into the new phase above 7.6 GPa before another allotrope, the well known β-Sn-type Ge(*tI*4), starts to form at 8.3(5) GPa. In the direction of decreasing pressures, the new modification is obtained at 6 GPa [2].

The crystal structure of the new allotrope Ge(*hR*8) can be described as a three-dimensional (3D) network formed by two crystallographically different types of four-bonded germanium atoms (Fig. 1). However, the apparent resemblance of the species is destroyed by pressure variation. Upon compression, the distances between the Ge1 atoms show a significantly stronger shortening than the other contacts (Fig. 2).

This experimental finding implies an alternative description of the crystal structure organisation. The atoms Ge2 form helices in direction of the crystallographic *c* axis, a partial structure which is similar to 1D building units in elemental α-selenium and α-tellurium, Se(*hR*3) and Te(*hR*3). These one-dimensional segments are interconnected by Ge2–Ge2 contacts into a 3D host framework which encloses channels oriented along the *c* axis. The other type of germanium atoms occupies the resulting tubular voids forming chains as guests, with alternating short and long interatomic distances.

In order to investigate the special partitioning of the crystal structure with quantum chemical methods, chemical bonding was analyzed by means of the electron localizability indicator [2]. Each short Ge–Ge contact exhibits an attractor in ELI evidencing four covalent bonds for both types of Ge atoms (Fig. 3). In contrast to other element modifi-

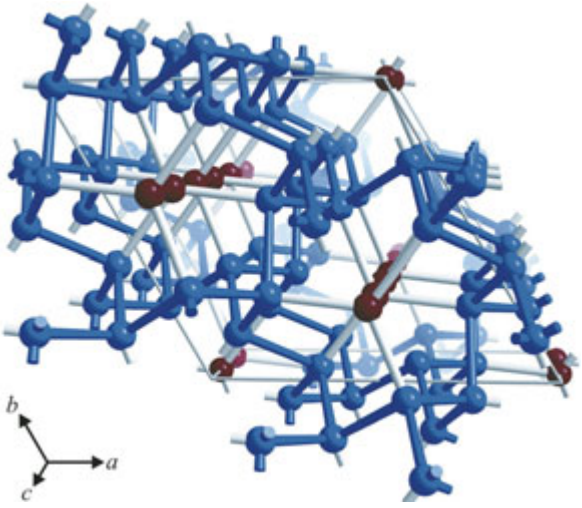

Fig. 1: Crystal structure of Ge(hR8). Crystallographically different germanium atoms are indicated by red (Ge1) and blue (Ge2) spheres, respectively.

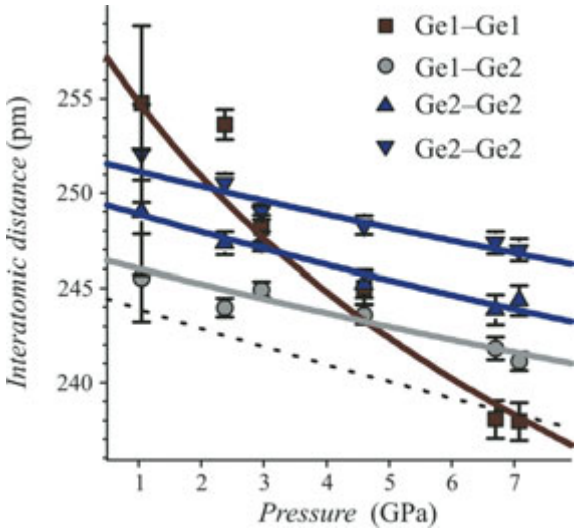

Fig. 2: Pressure-induced changes of interatomic distances in Ge(hR8). The dotted line indicates the distances in diamond-type germanium.

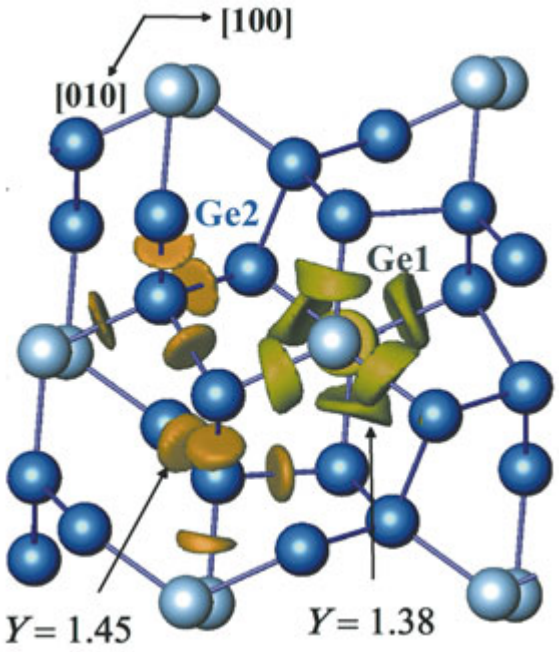

Fig. 3: Isosurfaces of the electron localizability indicator of Ge(hR8) revealing the four-bonded character of both types of germanium atoms [2].

cations with a similar structural host–guest organisation, the interactions within and between the partial structures of Ge(*hR*8) are equivalent [2]. The bonds connecting atoms of the network with atoms in the channels stabilize a normal periodic arrangement in Ge(*hR*8) while assemblies like K-III [3] or Sb-II [4] exhibit dissimilar identity periods of host and guest partial structures.

The covalent bonding in germanium allotropes impedes structural transformations at ambient temperature. Thus, the phase formation becomes controlled kinetically and upon pressure decrease to ambient conditions, germanium can form the metastable modification Ge(*tP*12), which also comprises two different types of four-bonded atoms (Fig. 4). The refinement of the positional parameters based on single-crystal X-ray diffraction intensities reveals interatomic distances *d*(Ge–Ge) covering a range from 248.07(8) pm to 250.53(6) pm [5]. They are significantly longer than *d*(Ge–Ge) of 245 pm in the stable diamond-type modification.

The 3D atomic arrangement contains helical chains (Fig. 4) which are similar to those observed in the recently solved high-pressure crystal structure of the element modification S(*tI*16) [6]. In Ge(*tP*12), four of these 1D segments are interconnected by bridging Ge1 atoms. In agreement with

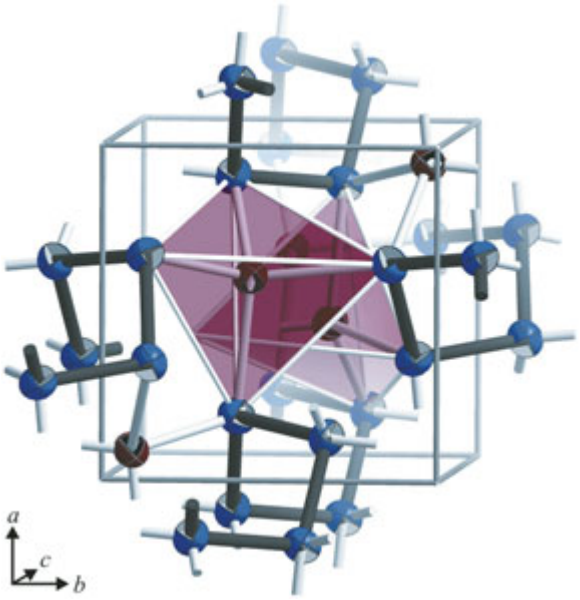

Fig. 4: Crystal structure of the metastable modification Ge(tP12). Crystallographically different germanium atoms are indicated by dark red and blue spheres, respectively.

the description implying low-dimensional building units, the compression of the modification Ge(*tP*12) is significantly higher perpendicular to the helices than parallel to the spiral direction.

Anionic frameworks of silicon and germanium

Strongly polar intermetallic compounds with silicon or germanium as a majority component form a diversity of frameworks. These binary phases constitute a class of fascinating materials with respect to electron counting schemes and physical properties. Several of these compounds feature thermoelectric or superconducting behaviour. The occurrence of these effects is often discussed in the context of interactions between network and filler atoms [7, 8].

Structural patterns of mainly four-bonding network atoms which are electron-precise according to the 8–*N* rule and the Zintl concept normally show semiconducting behaviour. In clathrate-type structures of germanium or tin, electrons donated by the cationic metals are accommodated in electron pairs around defects [9] or the charge is compensated by replacement of group 14 elements with group 13 atoms in the framework [10]. By contrast, silicon networks like those in compounds $M_{8-x}Si_{46}$ (*M* = Na, K; Ba) may hold a surplus of electrons and exhibit metallic conductivity [11].

In high-pressure high-temperature experiments performed with the aim to synthesize multinary silicon-rich cage compounds, the extreme conditions are realized with an octahedral multianvil device in combination with a hydraulic press. Pressure and temperature calibration is performed prior to the experiments.

A new structural pattern is observed for compositions close to $EuSi_6$ [12]. More systematic investigations reveal that the stability field can be extended to $EuSi_{6-x}Ga_x$. In the Eu–Si system, the formation of $EuSi_6$ has a low-pressure limit of 8(1) GPa. Subsequent high-pressure experiments with a mixture Ca–Si and Sr–Si evidence the formation of the isotypic compounds $CaSi_6$ above 10 GPa and $SrSi_6$ above 6 GPa [13,14].

In order to analyze the homogeneity ranges of the binary compounds MSi_6, we prepared three samples in each silicon-rich part of the phase diagrams. In case of silicon-poorer compositions like 1:5, we observe phases like MSi_2 together with MSi_6, for 1:6 we find pure MSi_6. In the silicon-richer mixtures, e.g., 1:12, MSi_6 is accompanied by elemental silicon. Moreover, the refined lattice parameters of each hexasilicide are found to be equal within three standard deviations at different compositions. These findings evidence constant compositions MSi_6 and exclude a significant homogeneity range with respect to defects in the silicon framework or in the metal partial structure.

The crystal structure of the high-pressure phases MSi_6 (M = Eu; Ca, Sr) is shown in Fig. 5. The atomic patterns which are isotypic to $EuGa_{2\pm x}Ge_{4\pm x}$ [15,16] comprise 3D frameworks of four-bonded silicon atoms $(4b)Si^0$. The electropositive metal atoms are located in large voids of this partial structure.

Upon heating at ambient pressure, exothermic, monotropic decompositions of the phases MSi_6 (M = Eu; Ca, Sr) into MSi_2 and Si indicate a metastable character at ambient conditions. Decomposition at low temperatures is prevented by the covalent bonding in the frameworks providing a sufficiently high energy barrier.

Regarding physical properties of $EuSi_6$, the magnetic susceptibility data (Fig. 6) indicate a Curie behaviour except at low temperatures (upper left inset of Fig. 6). The effective magnetic moment $\mu_{eff} = 8.09\ \mu_B$ obtained by a fit to the $\chi(T)$ data at temperatures above 20 K is consistent with the $^8S_{7/2}$ multiplet of europium with configuration $4f^7$

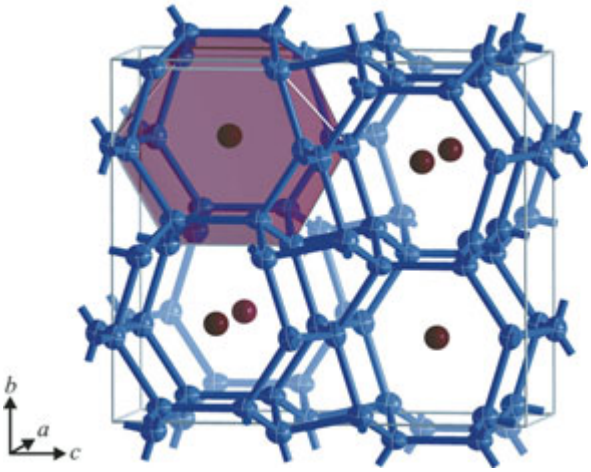

Fig. 5: Crystal structure of the high-pressure phases MSi_6 (M = Eu, Ca, Sr). Three crystallographically different silicon atoms form a three-dimensional network of four-bonded atoms (blue spheres). The metal atoms (red spheres) centre large voids.

(Eu^{2+}, $\mu_{free} = 7.94\ \mu_B$). The magnetic behaviour is quite complex at low temperatures. The Weiss parameter $\theta = -1.6$ K is negative and small indicating antiferromagnetic interactions. A kink at $T_N = 11.2$ K indicates an ordering of the europium $4f$ moments. This anomaly of $\chi(T)$ is followed by further discontinuities at lower temperatures.

Since europium is in the oxidation state +2, the phases MSi_6 hold an excess of two electrons per formula unit: $M^{2+}[(4b)Si^0]_6 \cdot 2e^-$. Accordingly, the resistivity $\rho(T)$ of $EuSi_6$ increases linearly with temperature for $T > 50$ K indicating a metal-type conductivity (lower right inset of Fig. 6). The absolute value of 1 mΩ cm at $T = 300$ K is above the classical limit for metallic conduction and classi-

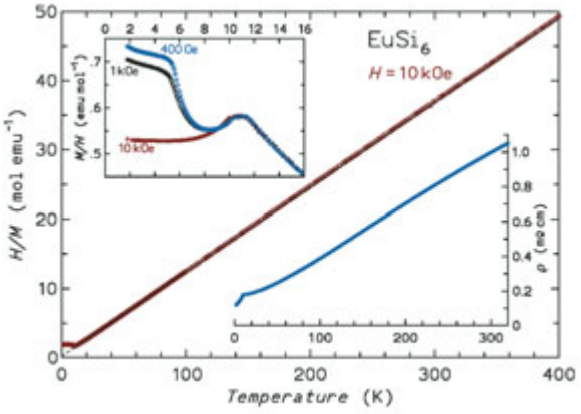

Fig. 6: Inverse magnetic susceptibility of $EuSi_6$ as a function of temperature (red symbols).The black line shows the Curie-Weiss fit. The inset upper left displays the susceptibility for different fields at temperatures below 16 K.

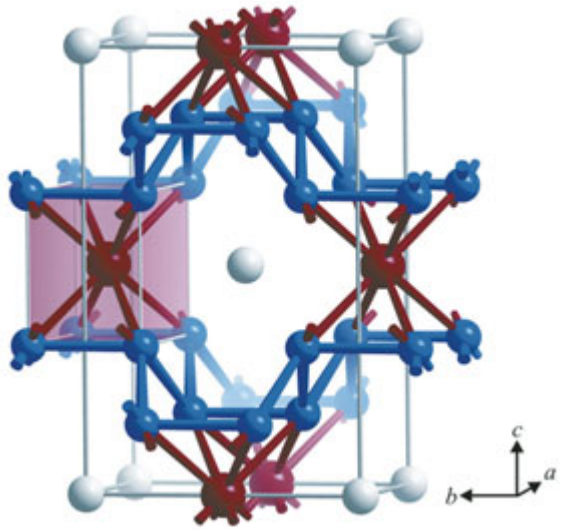

Fig. 7: Crystal structure of the high-pressure phases $REGe_5$ (RE = Nd, Gd, Sm, Ce). Germanium atoms in the corrugated sheets are displayed as blue spheres, eightfold coordinated Ge as red spheres, and the rare-earth metal is shown in white.

fies $EuSi_6$ as a bad metal. The discontinuous change of slope around 11 K is attributed to the magnetic ordering of the europium $4f^7$ ions.

The synthesis of a series of compounds with composition MSi_6 initiated a methodical study of the potential of chemical reactions at extreme conditions in stabilizing binary silicon- or germanium-rich compounds. Treatment of germanium-rich mixtures of the rare-earth metals Nd, Gd, Sm or Ce at extreme conditions evidences the formation of compounds $REGe_5$. The crystal structure is isotypic to recently characterized $LaGe_5$ [17] and comprises two types of germanium atoms (Fig. 7). One species forms corrugated nets, and between these two-dimensional building units rare-earth metal atoms are located in large cages. A second type of eightfold coordinated germanium atoms occupies smaller voids in the centre of a distorted germanium cube.

Conclusion

High-pressure high-temperature conditions stabilize a diversity of silicon and germanium structural patterns which are until now inaccessible at ambient pressure. The synthesis of several new binary silicon and germanium phases justifies further experiments to explore the potential of this method to realize new atomic arrangements of post-transitions elements and hitherto unknown compositions in the binary phase diagrams. The metastable character in combination with often extraordinary bonding features of these atomic motifs motivates an ongoing systematic research for novel and technologically useful combinations of physical properties in this class of materials.

References

[1] *A. M. Guloy, R. Ramlau, Z. J. Tang, W. Schnelle, M. Baitinger, and Yu. Grin,* Nature **443** (2006) 320.

[2] *U. Schwarz, A. Wosylus, B. Böhme, M. Baitinger, M. Hanfland, and Yu. Grin,* Angew. Chem. **120** (2008) 6895; Angew. Chem. Int. Ed. **47** (2008) 6790.

[3] *U. Schwarz, L. Akselrud, H. Rosner, A. Ormeci, Yu. Grin, and M. Hanfland,* Phys. Rev. B **67** (2003) 214101.

[4] *M. I. McMahon, R.J. Nelmes, U. Schwarz, and K. Syassen,* Phys. Rev. B **74** (2006) 140102.

[5] *O. Degtyareva, E. Gregoryanz, M. Somayazulu, P. Dera, H.-K. Mao, and R. J. Hemley,* Nature Mater. **4** (2005) 152.

[6] *A. Wosylus, Yu. Prots, W. Schnelle, M. Hanfland, and U. Schwarz,* Z. Naturforsch. **63b** (2008) 608.

[7] *G. A. Slack, in CRC Handbook of Thermoelectrics,* edited by D. M. Rowe, CRC Boca Raton, 1995.

[8] *K. Tanigaki, T. Shimizu, K. M. Itoh, J. Teraoka, Y. Moritomo, and S. Yamanaka,* Nature Mater. **2** (2003) 653.

[9] *H. G. von Schnering,* Nova Acta Leopoldina **59** (1985) 168.

[10] *B. Eisenmann, H. Schäfer, and R. Zagler,* J. Less-Common Met. **118** (1986) 43.

[11] *S. Yamanaka, E. Enishi, H. Fukuoka, M. Yasukawa, Inorg. Chem. **39** (2000) 56; B. Böhme, A. M. Guloy, Z. J. Tang, W. Schnelle, U. Burkhardt, M. Baitinger, and Yu. Grin,* J. Am. Chem. Soc. **129** (2007) 5348.

[12] *A. Wosylus, Yu. Prots, U. Burkhardt, W. Schnelle, U. Schwarz, and Yu. Grin,* Solid State Sciences **8** (2006) 773.

[13] *A. Wosylus, Yu. Prots, U. Burkhardt, W. Schnelle, and U. Schwarz,* Sci. Technol. Adv. Mater. **8** (2007) 383.

[14] *A. Wosylus, Yu. Prots, U. Burkhardt, W. Schnelle, U. Schwarz, and Yu. Grin,* Z. Naturforsch. **61b** (2006) 1485.

[15] *V. Pacheco, A. Bentien, W. Carrillo-Cabrera, S. Paschen, F. Steglich, and Yu. Grin,* Phys. Rev. B **71** (2005) 165205.

[16] *J. D. Bryan and G. D. Stucky,* Chem. Mater. **13** (2001) 253.

[17] *H. Fukuoka and S. Yamanaka,* Phys. Rev. B **67** (2003) 094501.

[1] European Synchrotron Radiation Facility, 6 rue Jules Horowitz, Grenoble, France.